American Mineralogist, Volume 75, pages 1059–1070, 1990

Temperature, size, and depth of the magma reservoir for the Taylor Creek Rhyolite, New Mexico

Wendell A. Duffield
Branch of Igneous and Geothermal Processes, U. S. Geological Survey, 2255 North Gemini Drive, Flagstaff, Arizona 86001, U.S.A.

Edward A. du Bray
U.S. Geological Survey, MS 905, Box 25046, Denver Federal Center, Denver, Colorado 80225, U.S.A.

Abstract

The 55 km³ mid-Tertiary Taylor Creek Rhyolite in southwestern New Mexico consists of 20 lava domes and flows. This rhyolite is metaluminous to weakly peraluminous and contains an average of 77.6 ± 0.4% SiO_2; Al_2O_3, Na_2O, and K_2O, the other major constituents, also vary little throughout the lava field. The Taylor Creek Rhyolite contains about 15–35 vol% phenocrysts, which are principally subequal amounts of quartz and sanidine accompanied by minor oligoclase and altered biotite or hornblende or both.

Compositional zonation in feldspar phenocrysts analyzed by electron microprobe is very minor and nonsystematic; most grains show less than 1 mol% Ab variation. In addition, the compositions of each feldspar species vary little throughout the suite of analyzed samples. This chemical homogeneity of phenocrysts reflects similar whole-rock homogeneity and suggests that the lavas were tapped from a single large reservoir of magma. Ages of sanidine phenocrysts determined using $^{40}Ar/^{39}Ar$ indicate that the Taylor Creek Rhyolite lavas were emplaced during a period of less than 0.42 m.y. and possibly less than 0.13 m.y., which is consistent with the single-reservoir scenario. Based on the distribution of vents for the lavas, it is inferred that the single reservoir was at least several hundreds of square kilometers in plan view.

Two-feldspar geothermometry suggests that Taylor Creek Rhyolite phenocrysts crystallized at about 775 °C, at an assumed pressure of 2 kbar. Fe-Ti-oxide geothermometry suggests phenocryst growth at about 800 °C. These temperatures are equal, within a conservative estimate of the uncertainties associated with the methods of determination, and they are consistent with fluid-inclusion-homogenization temperatures and ^{18}O-fractionation temperatures between about 700 °C and 800 °C for vapor-phase minerals deposited in the outer rinds of the lavas as they cooled, immediately following emplacement. A temperature of 800 °C for phenocryst growth in high-silica rhyolite magma suggests a volatile-poor (H_2O, F, Cl) system. Experimental studies suggest that quartz and potassium-feldspar crystals that grow from H_2O-undersaturated granitic magmas should exhibit resorption texture, a texture ubiquitous to Taylor Creek Rhyolite quartz and sanidine phenocrysts.

Insofar as experimental results in the system $NaAlSi_3O_8$-$KAlSi_3O_8$-SiO_2-H_2O are applicable to the Taylor Creek Rhyolite, a comparison between the natural and experimental systems indicates that Taylor Creek Rhyolite magma at 800 °C could have been saturated with H_2O and at or near the liquidus at a pressure of about 0.5 kbar. We tentatively conclude that the Taylor Creek Rhyolite magma was H_2O undersaturated and subliquidus at an unspecified pressure greater than 0.5 kbar during phenocryst growth and that Taylor Creek Rhyolite pyroclastic deposits formed because volatile saturation developed during the ascent of magma to sites of eruption.

Introduction

The Taylor Creek Rhyolite comprises a group of Tertiary lava domes and flows that crop out in the east-central part of the Mogollon-Datil volcanic field in New Mexico (Fig. 1). These rhyolite lavas are flow-foliated and moderately porphyritic, and with rare exception have a devitrified groundmass. Presumably because of their uniform appearance and the attendant difficulty in locating interflow contacts, the lavas were lumped into a single map unit (Fries and Butler, 1943) during the first comprehensive study of the area. Recently, successful subdivision into eruptive units indicates that at least 20 vents

0003–004X/90/0910–1059$02.00

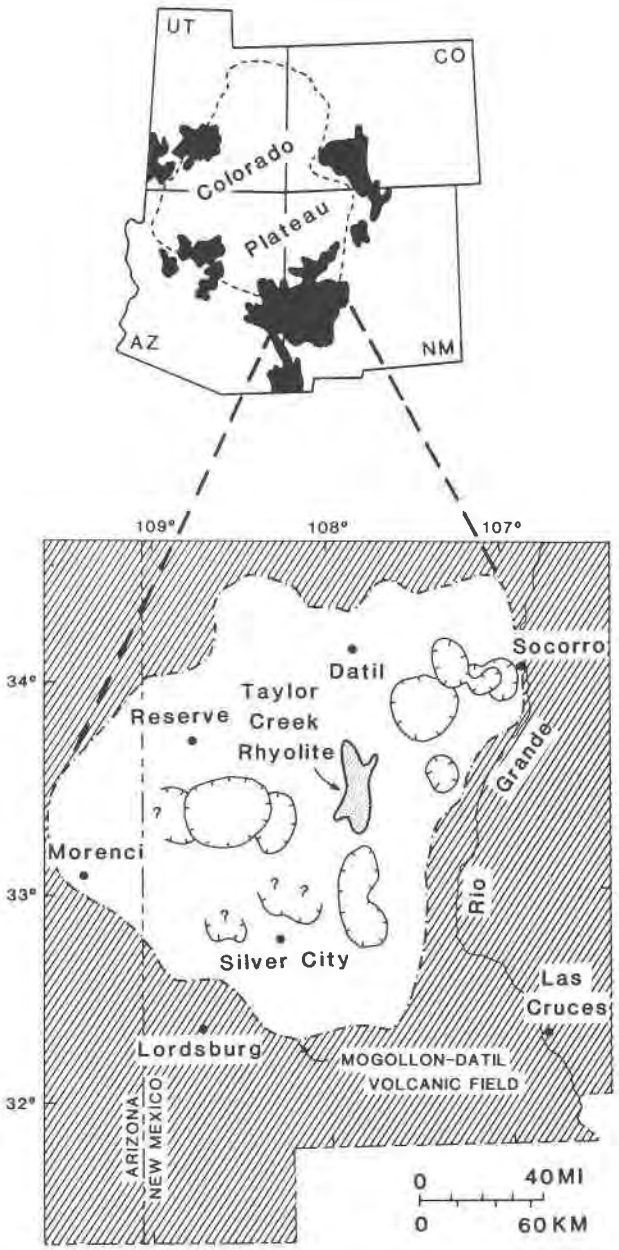

Fig. 1. Index maps showing Cenozoic volcanic fields (shaded areas, upper map) around the Colorado Plateau and the location of the Taylor Creek Rhyolite within the Mogollon-Datil volcanic field. Calderas shown by hachured lines.

were active during growth of the lava field (Duffield et al., 1987). These vents and the lavas emplaced from them are distributed within a rectangular area of several hundred square kilometers elongated to the north. Each vent appears to have been active only once and began with a pyroclastic phase that was followed by the growth of a lava dome or flow. The lavas appear to be roughly contemporaneous, based on a comparable minor degree of interflow erosion throughout the lava field, and all of them may have been emplaced in less than 130000 years, as indicated by high-precision $^{40}Ar/^{39}Ar$ age determinations (Dalrymple and Duffield, 1988). Major-element composition is constant or nearly so. Silica averages about 77.6 ± 0.4 wt%, and the other major constituents also vary little (W. A. Duffield, unpublished data); the rhyolite is metaluminous to weakly peraluminous.

The Taylor Creek Rhyolite has long been of special interest to geologists because it locally contains cassiterite-bearing veins and is the source of cassiterite-rich placer deposits, some of which have been mined intermittently since about the mid-1900s (Maxwell et al., 1986). The Sn of the cassiterite is interpreted to have come from the lavas themselves as they degassed, cooled, and devitrified immediately after emplacement (Correa, 1981; Lawrence, 1985; Eggleston, 1987; Duffield et al., 1987). Thus, knowledge of the time-space-composition relations that existed during the growth of the lava field and information about the magma reservoir from which eruptions were fed are essential to understanding the process of mineralization and the petrogenetic history of the lava field. Geologic mapping, determination of radiometric ages, studies of whole-rock trace-element chemistry, and modeling of Nd and Sr isotope systematics (Eggleston, 1987; Duffield et al., 1987; Duffield, in press; Dalrymple and Duffield, 1988; Reece et al., in press) have provided considerable information about the Taylor Creek Rhyolite magma and lava systems. Additional information about the temperature of Taylor Creek Rhyolite magma has been obtained from determination of the compositions of feldspar and Fe-Ti-oxide phenocrysts, as described herein.

Geology

The Mogollon-Datil, in southwestern New Mexico, is one of several Tertiary volcanic fields located around the margin of the Colorado Plateau physiographic province (Fig. 1). The pre-Tertiary sequence exposed adjacent to and near the Mogollon-Datil volcanic cover consists principally of Mesozoic and Paleozoic sedimentary rocks that overlie a Precambrian granitic and metamorphic complex. The volcanic field itself is an accumulation of mafic, intermediate, and silicic lava flows and pyroclastic rocks, mostly of mid-Tertiary age (Elston, 1984; Ratte, 1987), that encompasses roughly 10000 km^3. The field also includes several calderas that formed in response to large volume, rapid eruptions of magma emplaced as ash-flow sheets.

The Taylor Creek Rhyolite is located in the east-central part of the volcanic field. These lavas are sandwiched within the Mogollon-Datil ash-flow sequence, but they apparently are not directly related to any of the calderas, the nearest of which are tens of kilometers away. Most of the Taylor Creek lavas form domes that are roughly equidimensional in plan view, which indicates that lava erupted onto terrain of moderate or little relief and thus tended to spread radially away from vent areas. The bases of flows are observed or inferred to be at approximately

a common elevation, which further implies a low-relief, lava-emplacement surface and also indicates that little postemplacement tectonism has affected the region. A few northeast- and northwest-trending normal faults of basin and range and Rio Grande Rift affinities offset Taylor Creek Rhyolite locally. These faults and gentle regional westward tilting, indicated by a widespread westerly dip of about 10–20° in ash-flow sheets, appear to represent the only postvolcanic tectonism that has affected the area.

Most, if not all, eruptions of Taylor Creek magma began with a pyroclastic phase that produced a variety of products, including local ash flows, fallout deposits, and surge beds. The pyroclastic phase was followed by a relatively quiet effusion of magma that resulted in the growth of a lava dome or flow. The relative volumes of pyroclastic and lava rocks vary among eruptive units, although exposures do not permit accurate reconstruction to a preerosion condition in most instances. Exposures of most eruptive units give the impression that lava is more voluminous than its genetically related pyroclastic deposits, but this impression may be an artifact of the high erodibility of most pyroclastic materials. Some of the lavas have no known pyroclastic counterparts; these may have been removed by erosion or covered by lava or both.

Erosion has removed an unknown amount of rock from the tops of all the lava domes and flows, and the eroded debris forms an extensive sheet of rhyolite-rich alluvium that surrounds and partly buries most of the remaining rhyolite. Scattered remnants of flow-generated breccia locally mark the essentially uneroded margins along the steep flanks of several of the lavas and at the base of one, but most current exposures are limited to coherent flow-foliated rhyolite that represents interior parts of domes and flows. The thickest continuous vertical exposure of the rhyolite is nearly 300 m. Conservative reconstruction to preerosion conditions suggests that the volumes of domes and flows range from about 0.2 to 10.5 km^3, and that the 20 eruptive units cumulatively amount to about 55 km^3.

Petrography

Almost all of the Taylor Creek Rhyolite is flow foliated and has a devitrified groundmass. Vitrophyres are known at only about a half-dozen localities, and most are in pyroclastic phases of the rhyolite. Devitrification textures include spherulitic, plumose, and granular intergrowths of silica and alkali feldspar. These are the high-temperature products of devitrification that occurred as the rhyolite cooled to ambient temperature immediately after emplacement.

Phenocryst contents of the Taylor Creek Rhyolite lavas range from 12–38 vol%; most are between 15 and 35. Variations within individual eruptive units are small and probably within the uncertainty characteristic of stained-slab and thin-section modal analysis. Most phenocrysts are between 2 mm and 4 mm in maximum dimension; a few grains are as large as 7 mm. Measurements of phenocryst size in thin sections suggest a positive correlation between the volume of phenocrysts and grain size.

The phenocryst assemblage is dominated by subequal amounts of quartz and sanidine (Duffield et al., 1987). Quartz and sanidine occur as euhedral and subhedral grains. Most quartz and sanidine grains are partly rounded, and many exhibit deep smooth-walled embayments. Many sanidine grains appear optically homogeneous, whereas some show a microperthitic texture. Sanidine chatoyancy seen at some outcrops presumably is an effect of this texture. No sanidine grains appear optically zoned, which is consistent with the intragrain compositional homogeneity described later.

The third most abundant phenocryst phase is potassic oligoclase, which is present in amounts somewhat less than 1.5 vol%. Oligoclase generally is subhedral to anhedral and commonly occurs in glomeroporphyritic clots with sanidine. Sanidine forms overgrowths on some oligoclase grains. Oligoclase grains exhibit weak or no optical zonation, which is consistent with minor intragrain compositional zonation. The petrographic relations suggest that quartz, sanidine, and oligoclase grew in the same stable magmatic environment under equilibrium conditions.

In almost all thin sections examined, mafic phenocrysts, which account for less than 1.5 modal percent, are altered to a very fine-grained opaque material that may or may not preserve the original shape of the altered grain. Parts of some altered mafic phenocrysts exhibit the bird's-eye-maple extinction typical of mica, and a few others exhibit shapes suggestive of amphibole cleavage. Fresh grains of hornblende, and occasionally biotite in vitric samples, strongly suggest that the mafic phenocrysts in the devitrified rocks were indeed one or the other of these phases before alteration.

Locally, the lavas are unusually porous and friable. These localities are interpreted to mark relatively vesicular zones of high permeability that served as major channel ways for a vapor phase during degassing of newly emplaced, cooling lava. Because many rock-forming constituents are mobile within these zones of intense vapor flux (Smith, 1960), original magmatic rock compositions may be considerably altered there (Eggleston, 1987). We collected dense samples that crop out well away from the vapor-phase zones for our study, and we further checked samples in thin sections to avoid rocks with evidence of vapor-phase crystallization.

Analytical procedures

The major-oxide compositions of feldspar phenocrysts were analyzed at the U.S. Geological Survey in Denver, Colorado, using an ARL SEMQ electron microprobe equipped with six wavelength-dispersive spectrometers. A beam 25 μm wide was employed to mitigate the effects of microperthitic exsolution in sanidine and to minimize alkali loss. The sample current was 10 nA, and the accelerating voltage was 15 kV. Natural feldspars (Tiburon albite and OR-1A) and hematite were used as standards.

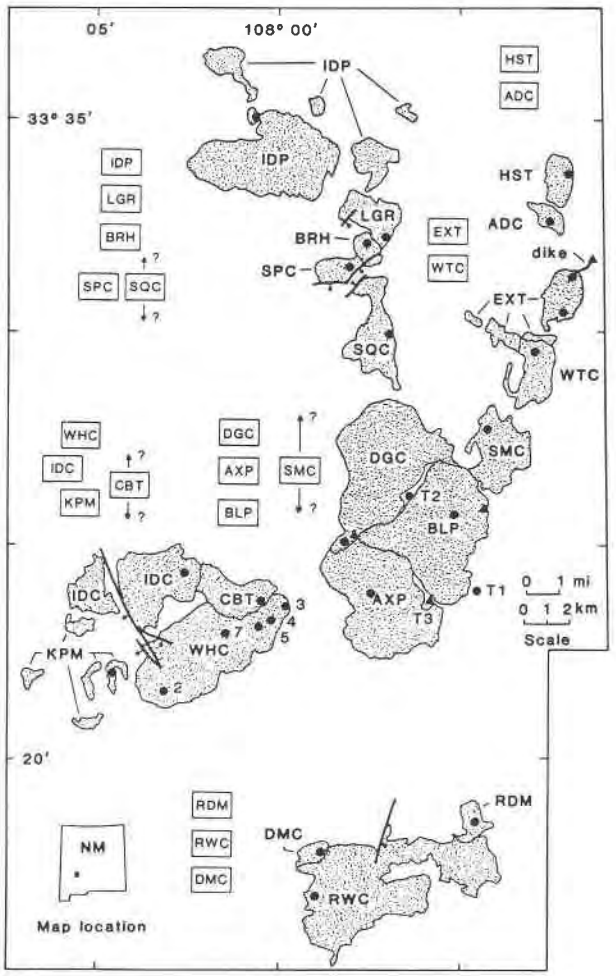

Fig. 2. Geologic map of the Taylor Creek Rhyolite, generalized after Duffield et al. (1987). Three-letter codes identify map units, which are equivalent to eruptive units. Each map unit is interpreted to represent lava from its own vent, which lies within the area of outcrop. Stratigraphic relations are summarized by boxes near groups of overlapping lavas. Relative ages of nonoverlapping lavas are unknown. Locations of samples for feldspar study shown by dots, and those for Fe-Ti-oxide study shown by triangles; the map-unit designations correspond with those in Tables 1, 2, 3, and 4.

Data were reduced by the methods of Bence and Albee (1968). Analytical uncertainties in wt% for single analyses are SiO_2, ±0.55; Al_2O_3, ±0.23; FeO, ±0.03; CaO, ±0.04 (sanidine) and ±0.12 (oligoclase); Na_2O, ±0.15 (sanidine) and ±0.20 (oligoclase); K_2O, ±0.07 (sanidine) and ±0.04 (oligoclase). These are 1σ counting errors, that is, the square root of the number of on-peak counts expressed as oxide wt%.

One sample was selected for feldspar analyses from each of the 20 Taylor Creek Rhyolite lava domes and flows mapped by Duffield et al. (1987). Four more samples (Fig. 2) from map-unit WHC of Duffield et al. (1987) were analyzed to test for intraflow compositional variation of phenocrysts. In addition, one sample from a dike of Taylor Creek Rhyolite interpreted to be part of the shallow feeder system for lava that it locally crosscuts and two samples of Taylor Creek Rhyolite tephra were selected for the feldspar study.

Within each sample, three 20-second analyses were completed on three sanidine and three oligoclase grains, at core, intermediate, and rim positions, to measure intragrain zonation. Thus, nine spots on sanidine and nine spots on oligoclase were analyzed in each sample. Analyzed grains were chosen randomly, except that crystals with some of their original euhedral outlines were analyzed in order to test confidently for core-to-rim zonation; few phenocrysts are anhedral. Analyses for BaO and SrO were attempted for each feldspar species in several samples, but concentrations of these elements are below the limits of detection, approximately 0.03 and 0.04 wt%, respectively. Whole-rock Ba and Sr contents for these rocks range from about 5–100 ppm and 3–20 ppm (Duffield, unpublished data), respectively. We report mean compositions and associated standard deviations for each analyzed sample (Table 1).

Fe-Ti oxides were analyzed at the U. S. Geological Survey in Menlo Park, California, using an ARL SEMQ electron microprobe. Scanning spectrometers were used for Al, Mn, and V determination, and fixed spectrometers were used for Fe, Ti, Ca, and Si. The sample current was 20 nA, the accelerating voltage was 15 kV, the beam diameter was about 5 μm, and the counting time was 10 s. Natural diopside and hematite and synthetic TiO_2, $MgAl_2O_4$, V_2O_5, and Mn_2O_3 were used as standards. Data were reduced by the methods of Bence and Albee (1968).

Feldspar compositions

On a ternary diagram (Fig. 3), the field defined by the 27 compositions (Table 1) of the more calcic of the two feldspar species straddles the boundary between oligoclase and anorthoclase. The mean of all 27 data points barely lies within the anorthoclase field at Ab 78, but we call all these feldspar grains oligoclase to stress their coexistence with sanidine. Most of the compositional variation in oligoclase is within the Ab and Or molecular components. Similarly, variation in the An content of sanidine is relatively small, whereas Ab varies from about 47 to 58, with a mean at Ab 52.

Examination of individual analyses, recast as molecular end-members, reveals as much variation within cores (and within rims) as between cores and rims for 49 of the 54 examples. The remaining five examples deviate little from this trend. Maximum rim-to-core compositional variation within the samples is 4.1 mol% Ab in oligoclase; Ab variation in most samples is ≤0.6 (Table 2). Maximum rim-to-core compositional variation for sanidine is 4.7 mol% Ab; Ab variation is less than 1 in most samples. Rim-to-core variation is monotonic in 20 of the 54 examples; in 12 of 27 oligoclase-sanidine pairs, one of the feldspars is monotonically zoned, whereas the other

is not. Of four monotonically zoned pairs, three exhibit opposite trends in sanidine compared with oligoclase.

The maximum variation of feldspar compositions within a single flow (Table 1, samples WHC/2, 3, 4, 5, 7) is somewhat less than the maximum variation throughout the entire suite of samples studied; both are small, though slightly greater than analytical uncertainty. A comparison of molecular end-member compositions of individual samples with those of the mean of all samples (see Table 1) indicates that most samples are indistinguishable from the mean, within the associated ranges of standard deviations; by such comparison, only about 30% of the samples differ from the mean by more than 1 mol%. Intra- and intersample variations represent some compositional differences, albeit minor, within the feldspar-phenocryst population of the Taylor Creek Rhyolite lava field.

The molecular proportions of Ab in the cores of oligoclase and sanidine grains correlate with whole-rock Rb (correlation coefficient of about 0.7), which in turn shows a similarly strong negative correlation with phenocryst abundance. Rb ranges from about 240–470 ppm throughout the lava field and serves as a convenient measure of chemical evolution (Duffield et al., 1987). A detailed examination of relations among trace elements, phenocryst abundance, and feldspar-phenocryst compositions is beyond the scope of this paper.

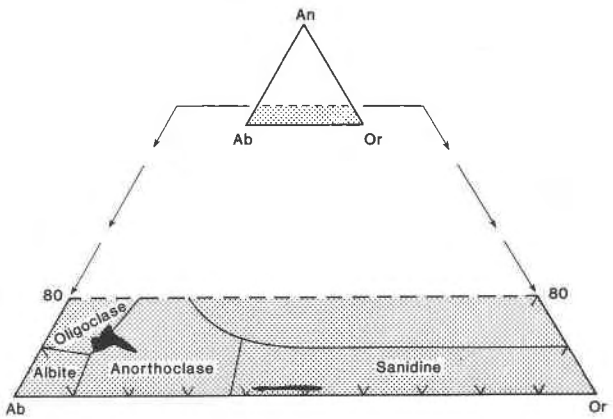

Fig. 3. Molecular proportions of feldspar phenocrysts in Taylor Creek Rhyolite. Black fields include 27 compositions each, calculated from data in Table 1.

Two-feldspar geothermometry

The partitioning of Na between pairs of feldspar phases that crystallize under equilibrium conditions is temperature and pressure dependent. Several expressions have been formulated for the calculation of crystallization temperature over ranges of pressure appropriate for crustal magma reservoirs (e.g., Stormer, 1975; Whitney and Stormer, 1977; Haselton et al., 1983; Price, 1985; Fuhrman and Lindsley, 1988); no two formulations yield the same results for a given set of analyses, although all are based on the experimental data of Seck (1971).

Two-feldspar temperatures (Table 3) were computed from the data in Table 1, using three different formulations. In a single sample, differences among these three formulations range from about 20–120 °C for the 27 feldspar pairs. We prefer the temperatures calculated from the geothermometer of Fuhrman and Lindsley (1988), principally because this geothermometer treats the feldspar system as a ternary and attempts convergence toward a common temperature for each of the three molecular end-members by a process of iterative solutions within a 2-mol% window that is assumed to reflect typical analytical imprecision. Thus, the technique not only yields a temperature for each molecular end-member, but with convergence it also suggests simultaneous feldspar crystallization under equilibrium conditions. All but five solutions (Table 3) for Taylor Creek Rhyolite feldspar pairs satisfy the equilibrium criteria of Fuhrman and Lindsley (1988), and four of the five anomalous samples barely violate the criteria. This evidence of equilibrium between feldspar-phenocryst species is consistent with the petrographic characteristics noted earlier.

Through the Fuhrman and Lindsley technique (1988), we also evaluated the effect of molecular Ab variation (Table 1) by calculating temperatures at the extremes of the compositional space defined by the standard deviations. Sample ADC was selected as a best case scenario (one of the smallest standard deviations for Ab), BLP as an average case, and WHC/4 as a worst case. ADC and BLP exhibit a maximum effect of 28 °C, with sums of differences that suggest equilibrium feldspar growth. WHC/4 exhibits solutions that indicate disequilibrium feldspar growth when Ab is maximized; the temperature calculated for the Or molecular is anomalously low. Thus, all or most solutions for each of the three tested samples converge toward a common temperature within the standard-deviation envelope. These results may be interpreted to indicate that standard deviations associated with the means reported in Table 1 have an insignificant effect on temperatures calculated by the Fuhrman and Lindsley (1988) technique. Temperatures so calculated for the grand mean of Table 1 also reflect this common result.

We calculated two-feldspar temperatures from core compositions to assess whether zoning, though apparently minor and nonsystematic, might produce different temperatures for core vs. the mean compositions reported in Table 1. The maximum temperature difference is 74 °C (Price geothermometer, sample EXT, Table 3), but almost all differences are less than 20 °C, far less than the uncertainty associated with any of the geothermometers. About half of the core temperatures are greater than those calculated from the mean compositions by the method of Fuhrman and Lindsley (1988), and about two-thirds are greater for the other two geothermometers. The lack of consistently greater (or lower) temperatures for core compositions agrees with our interpretation that zoning is nonsystematic and minor.

The effect of pressure on temperatures derived from

TABLE 1. Mean compositions ($n = 9$), standard deviations (in parentheses), mole proportions, and cations per 8 O atoms for feldspar phenocrysts

	AXP		DGC		BLP		SMC	
Map unit	O	S	O	S	O	S	O	S
SiO_2	64.91(0.62)	65.78(0.59)	66.45(0.45)	66.51(0.88)	65.98(0.42)	67.29(0.28)	65.26(0.61)	66.69(0.48)
Al_2O_3	21.33(0.53)	19.56(0.34)	20.99(0.33)	19.42(0.34)	21.18(0.16)	19.16(0.16)	21.22(0.18)	19.18(0.17)
Fe_2O_3*	0.18(0.02)	0.16(0.03)	0.20(0.02)	0.13(0.04)	0.13(0.03)	0.10(0.03)	0.14(0.03)	0.12(0.03)
CaO	2.15(0.14)	0.33(0.07)	2.20(0.16)	0.34(0.04)	2.11(0.17)	0.38(0.08)	2.12(0.12)	0.35(0.04)
Na_2O	9.36(0.16)	6.90(0.48)	9.01(0.10)	5.72(0.21)	9.27(0.24)	6.61(0.38)	9.69(0.16)	6.82(0.20)
K_2O	1.96(0.17)	7.82(0.41)	1.79(0.16)	8.21(0.31)	1.58(0.02)	7.00(0.42)	1.71(0.25)	7.23(0.20)
Total	99.89	100.55	100.64	100.33	100.25	100.54	100.14	100.39
				Mole proportions (%)				
An	10.03(0.70)	1.47(0.31)	10.65(0.73)	1.66(0.19)	10.00(0.62)	1.83(0.35)	9.79(0.52)	1.65(0.19)
Ab	79.06(0.66)	56.42(2.73)	79.03(0.44)	50.58(1.87)	80.91(1.36)	57.82(2.67)	80.83(1.13)	57.93(1.29)
Or	10.91(0.91)	42.11(2.74)	10.32(0.94)	47.75(1.76)	9.10(1.54)	40.35(2.85)	9.38(1.27)	40.42(1.35)
				Number of cations per 8 O atoms				
Z	4.000	3.990	4.005	4.008	4.006	4.001	3.996	3.994
X	1.018	1.063	0.969	0.982	0.979	0.985	1.028	1.020

	IDC		CBT		WHC/3		WHC/4	
	O	S	O	S	O	S	O	S
SiO_2	65.25(0.42)	66.62(0.36)	65.97(0.98)	66.51(0.47)	64.79(0.31)	66.28(0.47)	64.62(0.74)	66.23(0.93)
Al_2O_3	20.80(0.21)	18.42(0.27)	20.64(0.37)	18.63(0.11)	21.50(0.26)	19.37(0.19)	22.09(0.83)	19.39(0.71)
Fe_2O_3*	0.23(0.04)	0.14(0.04)	0.20(0.05)	0.12(0.03)	0.23(0.04)	0.17(0.03)	0.24(0.03)	0.16(0.04)
CaO	2.69(0.12)	0.35(0.08)	2.20(0.31)	0.33(0.04)	2.57(0.24)	0.34(0.04)	2.74(0.22)	0.36(0.06)
Na_2O	8.86(0.19)	5.76(0.14)	8.73(0.14)	5.79(0.18)	8.61(0.13)	5.06(0.20)	8.66(0.25)	5.58(0.35)
K_2O	1.56(0.13)	8.04(0.21)	2.09(0.33)	7.85(0.33)	1.89(0.27)	8.69(0.35)	1.80(0.38)	8.31(0.49)
Total	99.39	99.33	99.83	99.23	99.59	99.91	100.15	100.03
				Mole proportions (%)				
An	13.08(0.54)	1.71(0.42)	10.73(1.58)	1.65(0.20)	12.59(1.19)	1.71(0.20)	13.32(1.04)	1.78(0.27)
Ab	77.87(0.99)	51.26(1.08)	77.13(0.52)	51.97(1.67)	76.37(0.68)	46.15(1.81)	76.23(1.61)	49.61(2.83)
Or	9.04(0.75)	47.03(1.12)	12.14(1.83)	46.38(1.82)	11.04(1.56)	52.14(1.97)	10.45(2.22)	48.61(2.99)
				Number of cations per 8 O atoms				
Z	3.997	3.996	4.002	4.001	4.010	4.015	4.014	4.008
X	0.980	0.985	0.971	0.976	0.971	0.957	0.973	0.982

	WHC/5		WHC/2		KPM		IDP	
	O	S	O	S	O	S	O	S
SiO_2	64.00(0.93)	66.13(0.43)	65.03(0.85)	67.39(0.54)	65.84(0.57)	67.28(0.25)	65.35(0.27)	66.54(0.15)
Al_2O_3	22.75(0.50)	20.16(0.22)	21.01(0.14)	18.69(0.08)	21.12(0.47)	18.71(0.34)	20.89(0.17)	19.02(0.12)
Fe_2O_3*	0.24(0.03)	0.19(0.04)	0.23(0.03)	0.13(0.03)	0.22(0.06)	0.12(0.04)	0.13(0.03)	0.11(0.04)
CaO	2.41(0.11)	0.37(0.03)	2.65(0.17)	0.39(0.05)	2.52(0.36)	0.32(0.06)	2.14(0.15)	0.37(0.06)
Na_2O	8.86(0.21)	5.76(0.26)	8.71(0.18)	5.51(0.11)	9.03(0.17)	5.46(0.14)	9.11(0.45)	6.47(0.21)
K_2O	1.96(0.37)	7.87(0.37)	1.61(0.12)	8.06(0.23)	1.66(0.22)	8.61(0.25)	1.69(0.49)	7.03(0.22)
Total	100.22	100.48	99.24	100.17	100.39	100.50	99.30	99.54
				Mole proportions (%)				
An	11.42(0.80)	1.84(0.16)	13.04(0.77)	1.94(0.24)	12.11(1.72)	1.58(0.28)	10.38(1.07)	1.83(0.29)
Ab	77.34(1.70)	51.67(2.08)	77.54(1.19)	49.94(0.99)	78.40(0.90)	48.30(1.33)	79.92(2.02)	57.24(1.54)
Or	11.24(2.11)	46.49(2.14)	9.43(0.66)	48.11(1.17)	9.48(1.25)	50.12(1.26)	9.70(2.64)	40.94(1.43)
				Number of cations per 8 O atoms				
Z	4.024	4.021	4.004	4.004	4.000	3.999	4.004	4.002
X	0.984	0.965	0.969	0.956	0.983	0.980	0.983	0.985

	LGR		BRH		SPC		SQC	
	O	S	O	S	O	S	O	S
SiO_2	65.40(0.37)	66.94(0.15)	65.08(0.55)	66.33(0.26)	64.88(0.36)	65.95(0.26)	65.15(0.43)	66.42(0.37)
Al_2O_3	21.01(0.15)	19.03(0.13)	20.75(0.27)	19.05(0.13)	20.66(0.35)	19.09(0.11)	21.03(0.21)	18.89(0.19)
Fe_2O_3*	0.20(0.04)	0.17(0.03)	0.08(0.02)	0.07(0.04)	0.22(0.05)	0.13(0.03)	0.20(0.04)	0.14(0.04)
CaO	2.26(0.21)	0.43(0.05)	2.00(0.31)	0.39(0.06)	1.92(0.30)	0.42(0.06)	2.24(0.14)	0.41(0.07)
Na_2O	9.13(0.32)	6.42(0.29)	8.61(0.28)	5.81(0.28)	8.54(0.34)	5.94(0.16)	9.05(0.13)	5.68(0.24)
K_2O	1.79(0.44)	7.29(0.36)	2.53(0.58)	7.71(0.36)	2.97(0.50)	7.91(0.24)	2.30(0.09)	8.46(0.36)
Total	99.79	100.28	99.05	99.36	99.19	99.44	99.97	100.00
				Mole proportions (%)				
An	10.82(0.92)	2.09(0.21)	9.71(1.56)	1.95(0.30)	9.18(1.42)	2.06(0.31)	10.48(0.56)	1.99(0.33)
Ab	78.99(2.32)	56.04(2.21)	75.67(2.27)	52.33(2.22)	73.91(2.26)	52.20(1.31)	76.71(0.67)	49.51(2.07)
Or	10.19(2.55)	41.87(2.29)	14.62(3.36)	45.71(2.33)	16.91(2.92)	45.74(1.41)	12.81(0.43)	48.51(2.10)
				Number of cations per 8 O atoms				
Z	4.001	3.999	4.004	4.007	4.001	4.001	3.996	3.996
X	0.992	0.992	0.986	0.970	1.003	0.997	1.014	1.002

TABLE 1.—*Continued*

	HST		ADC		EXT		WTC	
	O	S	O	S	O	S	O	S
SiO_2	65.24(0.30)	66.83(0.31)	65.00(0.43)	66.06(0.41)	65.77(0.32)	66.81(0.35)	64.61(0.61)	65.99(0.26)
Al_2O_3	20.94(0.15)	18.73(0.21)	21.11(0.18)	19.06(0.12)	21.19(0.22)	19.17(0.12)	21.00(0.50)	18.92(0.14)
Fe_2O_3*	0.22(0.04)	0.17(0.04)	0.17(0.01)	0.12(0.02)	0.16(0.04)	0.10(0.03)	0.18(0.03)	0.13(0.04)
CaO	2.52(0.16)	0.30(0.04)	2.19(0.17)	0.36(0.04)	2.23(0.18)	0.34(0.04)	2.42(0.52)	0.39(0.06)
Na_2O	9.47(0.10)	5.78(0.21)	8.90(0.14)	6.22(0.23)	8.97(0.77)	6.39(0.20)	8.68(0.30)	5.60(0.29)
K_2O	1.60(0.10)	8.58(0.31)	2.27(0.10)	7.57(0.02)	1.36(0.30)	7.42(0.15)	2.37(0.37)	8.41(0.29)
Total	99.99	100.39	99.64	99.39	99.68	100.23	99.26	99.44
				Mole proportions (%)				
An	11.67(0.68)	1.43(0.17)	10.40(0.78)	1.75(0.19)	10.93(1.51)	1.65(0.19)	11.61(2.68)	1.89(0.29)
Ab	79.48(0.75)	49.85(1.75)	76.71(0.59)	54.58(1.65)	81.00(2.36)	55.74(1.12)	74.95(1.20)	49.34(1.93)
Or	8.85(0.58)	48.72(1.67)	12.89(0.62)	43.67(1.55)	8.08(1.79)	42.61(1.13)	13.43(1.97)	48.77(2.12)
				Number of cations per 8 O atoms				
Z	3.990	3.993	4.002	4.001	4.003	4.003	3.998	4.000
X	1.023	1.008	1.001	0.998	0.989	0.988	1.003	0.996

	WHC/7		RWC		RDM		DMC	
	O	S	O	S	O	S	O	S
SiO_2	66.56(0.42)	66.29(0.64)	64.89(0.85)	66.67(0.24)	65.95(0.28)	66.97(0.38)	64.98(0.32)	66.15(0.30)
Al_2O_3	20.95(0.21)	19.19(0.17)	21.39(0.64)	18.94(0.18)	21.16(0.31)	19.16(0.29)	21.05(0.29)	18.70(0.14)
Fe_2O_3*	0.17(0.02)	0.14(0.04)	0.21(0.04)	0.16(0.04)	0.17(0.04)	0.09(0.04)	0.20(0.03)	0.11(0.03)
CaO	2.05(0.14)	0.32(0.05)	2.98(0.67)	0.43(0.06)	1.90(0.17)	0.25(0.05)	2.53(0.28)	0.32(0.05)
Na_2O	9.27(0.17)	5.99(0.17)	8.60(0.19)	5.95(0.20)	9.30(0.13)	6.16(0.24)	8.56(0.15)	5.10(0.20)
K_2O	1.70(0.35)	7.63(0.21)	1.64(0.43)	7.67(0.37)	1.67(0.19)	7.59(0.40)	2.00(0.29)	8.84(0.24)
Total	100.70	99.56	99.71	99.82	100.15	100.22	99.32	99.22
				Mole proportions (%)				
An	9.82(0.68)	1.54(0.24)	14.50(3.21)	2.11(0.30)	9.18(0.80)	1.21(0.27)	12.40(1.29)	1.61(0.23)
Ab	80.46(1.33)	53.55(1.33)	75.95(1.54)	52.99(1.87)	81.24(0.87)	54.58(2.25)	75.93(0.77)	45.98(1.52)
Or	9.72(2.00)	44.91(1.34)	9.55(2.54)	44.90(2.05)	9.58(1.03)	44.20(2.19)	11.67(1.72)	52.41(1.61)
				Number of cations per 8 O atoms				
Z	4.003	4.008	4.002	4.002	4.009	4.006	4.004	4.003
X	0.979	0.977	0.974	0.979	0.978	0.978	0.973	0.976

	T1		T2		Dike		Grand mean	
	O	S	O	S	O	S	O	S
SiO_2	65.35(0.53)	65.99(0.63)	63.95(0.66)	66.09(0.58)	65.21(0.34)	66.45(0.34)	65.24(0.63)	66.49(0.43)
Al_2O_3	21.37(0.33)	19.28(0.24)	22.70(0.40)	19.48(0.74)	20.80(0.16)	18.68(0.12)	21.21(0.53)	19.08(0.36)
Fe_2O_3*	0.20(0.03)	0.13(0.03)	0.23(0.04)	0.17(0.05)	0.19(0.02)	0.12(0.03)	0.19(0.04)	0.13(0.03)
CaO	2.24(0.22)	0.30(0.06)	2.49(0.37)	0.40(0.18)	2.32(0.18)	0.33(0.04)	2.33(0.26)	0.36(0.04)
Na_2O	9.32(0.22)	5.78(0.26)	9.37(0.45)	5.39(0.21)	8.90(0.17)	5.85(0.23)	8.98(0.32)	5.91(0.47)
K_2O	1.85(0.37)	8.61(0.13)	1.77(0.39)	8.44(0.58)	1.87(0.22)	7.90(0.35)	1.89(0.35)	7.95(0.51)
Total	100.33	100.09	100.51	99.97	99.29	99.33	99.84	99.92
				Mole proportions (%)				
An	10.49(1.00)	1.41(0.26)	11.57(1.61)	1.99(0.91)	11.24(0.81)	1.60(0.19)	11.15(1.35)	1.74(0.23)
Ab	79.18(1.26)	49.75(1.32)	78.63(2.04)	48.30(2.13)	77.98(0.82)	52.09(1.97)	78.06(1.99)	52.11(3.38)
Or	10.32(2.10)	48.85(1.47)	9.80(2.30)	49.71(3.00)	10.78(1.35)	46.30(2.06)	10.79(1.96)	46.16(3.38)
				Number of cations per 8 O atoms				
Z	4.001	4.000	4.013	4.011	4.001	4.000	4.004	4.003
X	1.007	1.014	1.020	0.974	0.985	0.984	0.989	0.988

Note: See Figure 2 for sample locations and text for description of analytical procedures. Samples T1 and T2 are tephra that are tentatively correlated with eruptions that produced lavas AXP and DGC, respectively. Fe_2O_3* is total Fe reported as Fe_2O_3. The grand mean is calculated for $n = 27$. O = oligoclase and S = sanidine. *X* and *Z* are total cations (based on 8 O atoms) for the alkali metal and tetrahedral sites, respectively.

two-feldspar geothermometry was examined by calculating temperatures for selected samples at 0.5, 2, 5, and 10 kbar. Temperatures increase by as much as 150 °C between 0.5 and 10 kbar. However, 10 kbar corresponds to a crustal depth that may be too great for the Taylor Creek Rhyolite magma reservoir. Although we have no independent evidence to accurately define pressure, we believe that the depth to the top of the reservoir was more nearly akin to the pressure equivalent of 2 kbar than 10, and thus temperatures calculated for 2 kbar are interpreted to approximate the temperatures at which feldspar phenocrysts of the Taylor Creek Rhyolite grew. The mean at 2 kbar is 775 °C (Table 3) for results computed by the method of Fuhrman and Lindsley (1988). Calculated temperatures increase by about 10–20 °C per additional kbar, which is only about half the uncertainty associated with the Fuhrman and Lindsley (1988) method for a single temperature.

A histogram of calculated temperatures identified by sample exhibits a roughly normal distribution about the mean; no correlation is apparent between temperature and geographic position of samples (Figs. 4 and 2). Also,

TABLE 2. Summary of chemical zonation in feldspar phenocrysts, as measured by electron microprobe

Map unit/ sample no.	Oligoclase				Sanidine			
	Ab variation monotonic?	(Rim minus core)			Ab variation monotonic?	(Rim minus core)		
		Ab	Or	An		Ab	Or	An
WHC/2	N	0.0	0.2	−0.2	Y	0.9	−1.1	0.2
WHC/3	Y	−0.4	−0.2	0.6	N	−0.4	0.5	−0.1
WHC/4	N	−0.2	−0.2	0.4	N	4.7	−4.8	0.1
WHC/5	N	1.3	−1.8	0.5	Y	0.8	−0.7	−0.1
WHC/7	N	2.2	−3.2	0.9	N	1.2	−1.2	−0.1
CBT	Y	0.1	0.5	−0.6	N	1.6	−1.7	0.1
IDC	N	−0.3	0.8	−0.6	N	0.2	−0.2	0.1
KPM	N	0.5	0.5	−1.0	N	−1.0	0.7	0.3
DGC	Y	0.1	0.5	−0.7	N	−0.6	0.4	0.2
AXP	Y	−0.4	0.1	0.3	N	0.1	−0.6	0.5
BLP	Y	2.0	−2.7	0.7	N	1.8	−1.8	0.0
SMC	N	0.6	0.1	−0.7	Y	−1.1	1.3	−0.2
IDP	Y	1.7	−1.0	−0.6	Y	−0.7	0.9	−0.2
LGR	Y	1.7	−2.5	0.6	Y	−1.6	1.5	0.0
BRH	N	0.0	1.4	−1.4	Y	3.8	−4.3	0.5
SPC	N	1.9	−0.1	−1.7	N	−0.9	1.0	−0.1
SQC	Y	−1.0	0.0	0.9	Y	1.0	−1.0	0.0
HST	N	−0.1	0.7	−0.6	Y	−3.1	2.9	0.2
ADC	N	−0.4	−0.1	0.5	N	0.7	−0.8	0.1
EXT	Y	4.1	−0.7	−3.4	N	0.1	−0.1	0.0
WTC	N	0.4	−0.3	−0.1	N	0.4	−0.1	−0.3
DIKE	N	0.6	−1.3	0.7	N	−1.1	1.2	−0.1
RWC	N	1.0	1.4	−2.5	N	2.4	−2.3	−0.1
RDM	N	−0.1	0.3	−0.2	N	1.9	−2.1	0.2
DMC	N	0.3	0.2	−0.4	N	−0.2	0.2	−0.1
T1	Y	−0.8	0.4	0.5	Y	−0.5	0.8	−0.2
T2	Y	1.4	0.6	−2.0	N	−0.1	−0.1	0.2

Note: Amounts in mol%, calculated from means ($n = 3$) of core, intermediate, and rim positions. See text for discussion of analytical procedures and Figure 2 for sample locations. Samples T1 and T2 are tephra that are tentatively correlated with eruptions that produced lavas AXP and DGC, respectively. Y = yes. N = no.

a plot of whole-rock Rb vs. two-feldspar temperature and comparison of temperatures and relative ages of lavas exhibit no apparent correlations. The range of 95 °C in calculated temperatures is not much more than the uncertainty of ±40 °C for a single sample that Fuhrman and Lindsley attach to their method, although some of this range presumably reflects real though small compositional variation. We interpret 775 °C ± 40 °C as the approximate temperature at which feldspar phenocrysts crystallized from Taylor Creek Rhyolite magma.

Fe-Ti oxides

We searched for fresh coexisting magmatic magnetite and ilmenite in polished thin sections of all seven available samples of vitric Taylor Creek Rhyolite and of two samples of the devitrified counterparts. Magnetite is universally coarsely exsolved in the devitrified rocks, such that it was not possible to analyze exsolution lamellae for reconstruction of an average pre-exsolution composition. Magnetite grains in three of the seven vitrophyres are similarly coarsely exsolved, whereas the remaining four samples contain homogeneous crystals that yielded compositions interpreted to reflect magmatic conditions. Coexisting grains of ilmenite in these four samples also are quite homogeneous and, with one exception, exhibit little or no core-to-rim zoning.

Magnetite and ilmenite grains are subhedral to euhedral and average about 60 μm in cross section. Equilibrium pairs of magnetite and ilmenite, used in the temperature calculations, were selected principally on the basis of satisfying the Mg-Mn partitioning criterion for equilibrium suggested by Bacon and Hirshmann (1988). Low totals for recalculated (Stormer, 1983) magnetite analyses for all but sample DGC presumably are the result of fine-scale oxidation manifested by delicate trellis patterns on high-magnification SEM backscattered electron images. As Fe_{total}/Ti ratios are unaffected by such oxidation, calculated temperatures are believed to be accurate.

Two of the vitric samples (DGC and BLP, Table 4) that contain Fe-Ti oxides suitable for geothermometry are from lava flows. Almost all analyzed grains in these rocks form a tight cluster for each phase on Mn/Mg vs. Fe_{total}/Ti plots. One magnetite-ilmenite pair within the clusters consists of touching grains. Rare grains that plot away from the clusters may be xenocrysts.

Sample T3 is from a pyroclastic deposit of Taylor Creek Rhyolite. This sample contains many broken crystals and a variety of magnetite and ilmenite compositions. However, within individual glassy fragments in the sample, the dominant Fe-Ti oxide population has Mn/Mg and Fe_{total}/Ti essentially the same as those for the samples from lava flows described above and, hence, similar calculated temperature and f_{O_2}.

A sample from the chilled margin of a dike of Taylor

TABLE 3. Temperatures (°C) calculated for two-feldspar geothermometers, at 2 kbar

Map unit/ sample number	P	W & S	F & L	SOD
WHC/2	834(834)	808(820)	771(750)	61(30)
WHC/3	817(817)	797(797)	799(767)	29(21)
WHC/4	861(830)	834(806)	808(773)	48(47)
WHC/5	856(851)	834(830)	803(777)	48(41)
WHC/7	805(833)	790(808)	762(796)	70(77)
CBT	863(857)	843(837)	802(800)	38(42)
IDC	847(853)	820(823)	791(770)	75(82)
KPM	807(831)	787(809)	756(766)	63(64)
DGC	809(815)	792(797)	747(776)	40(55)
AXP	869(877)	849(856)	773(748)	66(62)
BLP	830(832)	810(816)	732(744)	82(63)
SMC	833(842)	814(821)	750(734)	86(94)
IDP	848(866)	826(840)	745(750)	87(76)
LGR	851(883)	828(859)	755(795)	67(54)
BRH	886(860)	869(846)	810(771)	18(9)
SPS	923(970)	907(950)	822(813)	5(16)
SQC	832(823)	816(808)	773(768)	16(18)
HST	804(826)	785(803)	746(773)	70(84)
ADC	900(890)	878(870)	803(804)	36(40)
EXT	815(889)	794(852)	753(754)	103(113)
WTC	872(861)	851(842)	794(795)	16(13)
DIKE	849(860)	828(838)	790(786)	58(63)
RWC	911(924)	870(877)	790(800)	84(83)
RDM	806(808)	792(794)	727(724)	67(100)
DMC	825(827)	805(807)	778(801)	20(13)
T1	790(812)	772(790)	757(755)	51(53)
T2	805(787)	790(772)	775(729)	48(53)
Mean	843(850)	822(828)	775(771)	
SD	35(38)	33(36)	26(24)	

Note: Calculations use data reported in Table 1 and mean core compositions (in parentheses). See Figure 2 for sample locations. P = Price, 1985. W & S = Whitney and Stormer, 1977 (model 1, sanidine). F & L = Fuhrman and Lindsley, 1988. SD = standard deviation. SOD = sum of differences associated with solutions to the F & L geothermometer; if SOD ≤ 80, the two feldspar species are interpreted to have grown in equilibrium (Fuhrman and Lindsley, 1988).

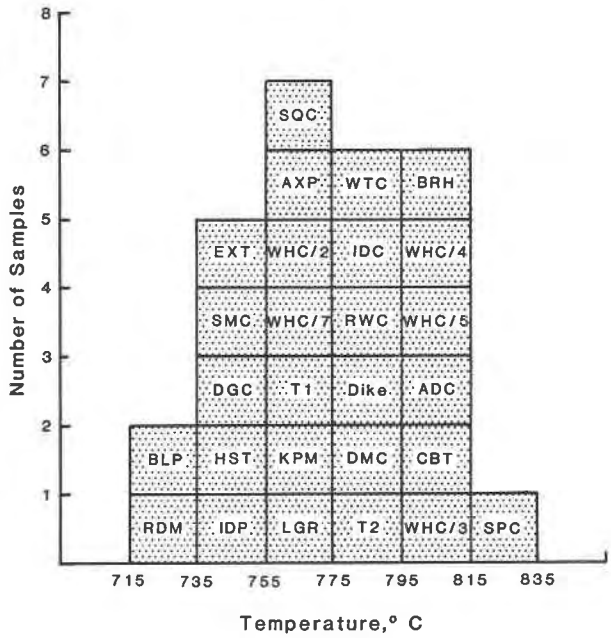

Fig. 4. Histogram of two-feldspar geothermometer temperatures (Fuhrman and Lindsley, 1988) at 2 kbar for Taylor Creek Rhyolite, calculated from data in Table 1. See Figure 2 for sample locations. The height of a sample within a column reflects its temperature relative to other samples in that column.

Creek Rhyolite (Table 4, Dike) contains appreciably zoned Fe-Ti oxides. The Fe_{total}/Ti ratio tends to increase toward the rims of grains, which may reflect partial equilibration at lower temperatures, as the rock cooled relatively slowly in the shallow subsurface. Temperatures (Andersen and Lindsley, 1988) calculated for core compositions are as high as 828 °C. We report data for grain margins in Table 4. A few Fe-Ti oxide grains with aberrant compositions may be xenocrysts.

All of the reported results plot near the magnetite-quartz-fayalite buffer curve, indicative of relatively nonoxidizing conditions and similar to most so-called topaz rhyolites (Christiansen et al., 1986). Temperatures reported for the vitric samples range from 798–819 °C (Table 4). Temperatures calculated from the population of oxides in three of the four samples suitable for geothermometry are approximately 800 °C at log f_{O_2} of −14. Temperatures of about 775 °C ± 40 °C calculated from the preferred two-feldspar geothermometer are compatible with these Fe-Ti-oxide results.

DISCUSSION

Temperatures calculated from the phenocryst geothermometers are consistent with lava-emplacement temperatures indirectly deduced from fluid inclusions in minerals that grew from vapor emitted by Taylor Creek Rhyolite lavas as they cooled. For example, Eggleston and Norman (1986) and Eggleston (1987) reported temperatures of fluid-inclusion homogenization somewhat higher than 700 °C in vapor-phase topaz, silica, and cassiterite. Rye et al. (in press) report temperatures of quartz and hematite growth in miarolitic cavities of Taylor Creek Rhyolite of about 800 °C, based on ^{18}O fractionation. Presumably, the temperature of lava emplacement and thus the maximum temperature of mineral deposition from a vapor phase would have been somewhat lower than the 800 °C at which we conclude the phenocrysts crystallized.

High-precision $^{40}Ar/^{39}Ar$ age determinations for two of the regional ash-flow sheets of the Mogollon-Datil volcanic field, one just beneath the Taylor Creek Rhyolite lavas and the other just above, indicate that these lavas were emplaced during a period of no more than 0.42 m.y. (McIntosh et al., 1986). Other $^{40}Ar/^{39}Ar$ ages on sanidine phenocrysts from six of the 20 Taylor Creek Rhyolite lavas mapped by Duffield et al. (1987) indicate that these lavas were emplaced during a period of about 0.13 m.y. or less (Dalrymple and Duffield, 1988); we speculate that the entire lava field formed during ≤0.13 m.y., a speculation that is being tested by determining $^{40}Ar/^{39}Ar$ ages for sanidine phenocrysts from all 20 mapped units. The idea that the lava field grew in such a geologically short period of time is consistent with field evidence. Relative

TABLE 4. Selected microprobe analyses of Fe-Ti oxides with calculated temperatures and f_{O_2}

	Map unit				
	DGC	BLP1	BLP	T3	Dike
			Magnetite		
SiO_2	0.19	0.06	0.26	0.16	0.19
Al_2O_3	0.81	0.69	0.83	0.81	0.90
FeO*	80.4	79.0	78.0	78.0	76.6
MgO	0.18	0.35	0.37	0.27	0.30
CaO	0.01	0.00	0.00	0.00	0.02
MnO	1.78	1.67	1.77	1.69	1.86
TiO_2	11.46	12.28	12.07	11.42	11.48
V_2O_3	0.03	0.01	0.02	0.02	0.04
Total	94.86	94.06	93.32	92.37	91.39
Fe_2O_3**	45.18	43.41	42.62	43.48	42.45
FeO**	39.74	39.94	39.65	38.87	38.41
Total	99.38	98.41	97.59	96.72	95.65
			Ilmenite		
SiO_2	0.03	0.06	0.12	0.03	0.07
Al_2O_3	0.05	0.03	0.04	0.05	0.03
FeO*	47.6	47.4	47.2	46.0	44.8
MgO	0.35	0.75	0.70	0.74	0.79
CaO	0.00	0.01	0.02	0.02	0.01
MnO	3.37	3.17	3.17	3.68	5.07
TiO_2	48.00	47.9	47.9	47.9	48.4
V_2O_3	0.03	0.00	0.03	0.01	0.02
Total	99.43	99.32	99.18	98.43	99.19
Fe_2O_3**	9.38	9.80	9.41	8.85	8.61
FeO**	39.16	38.58	38.73	38.04	37.05
Total	100.37	100.30	100.12	99.32	100.05
Xusp†	0.331	0.354	0.355	0.338	0.345
Xil†	0.907	0.902	0.906	0.910	0.912
T°C‡	800	819	813	798	798
$\log_{10} f_{O_2}$‡	−13.9	−13.5	−13.6	−14.0	−14.0

Note: Sample T3 is tephra tentatively correlated with the eruption that produced lava AXP. See Figure 2 for sample locations. BLP1 denotes results for a single pair of touching grains within sample BLP.

* = total Fe as FeO.

** Calculated from analysis, assuming stoichiometry (Stormer, 1983).

† Mole fractions calculated by the method of Stormer (1983).

‡ Determined by the method of Andersen and Lindsley (1988).

ages generally can be determined for pairs of lavas that overlap in the field, and in such instances one finds no evidence of substantial erosion between the lavas. On the contrary, the plan-view shape of the younger of overlapping lavas commonly appears to be controlled by the unmodified form of the flow or dome against which it banked. If our tentative conclusion about the maximum lifespan of the lava field is correct, the average interval between eruptions was less than about 6000 years.

A theoretical model of Smith and Shaw (1979) for reservoirs of silicic magma cooling within the upper crust, either conductively or by a combination of conduction and convection, indicates that the residual magma body left in the crust after eruption of the Taylor Creek Rhyolite would cool nearly to solidus temperature within about 100 000 years. This period is about the same as the inferred maximum lifespan of the lava field. Thus, it is reasonable to conclude, on the basis of these thermal considerations alone, that eruptions of Taylor Creek Rhyolite magma could have been fed from a single reservoir.

Many chemical and physical data are consistent with this single-reservoir scenario. The lavas are of nearly constant major-element composition, and they contain the same suite of phenocrysts, which are present in nearly constant proportions (Duffield, in press). As reported herein, each feldspar-phenocryst species is of nearly invariant composition throughout the lava field. In addition, the Taylor Creek area is within a few tens of kilometers of and partly surrounded by several mid-Tertiary calderas, some older and some younger than the Taylor Creek Rhyolite (McIntosh et al., 1986) and each of which formed by collapse when part of the magma in an underlying large-volume reservoir was erupted to feed an ash-flow sheet. On the assumption that the magma rose more or less vertically to sites of eruption, the proposed Taylor Creek Rhyolite magma reservoir was at least equal in plan-view size to the nearby Mogollon-Datil calderas. However, in contrast to the apparently volatile-rich caldera-producing magmas in the penecontemporaneous large reservoirs, Taylor Creek Rhyolite magma may have been too volatile-poor to have been erupted in a single large-volume pyroclastic event and instead leaked to the surface to feed multiple eruptions that produced mostly lava domes and flows.

Alternatively, Taylor Creek Rhyolite lava domes and flows may have been fed from a series of independent reservoirs or magma batches. This scenario requires that magmas of nearly constant major-element composition and temperature, and of nearly constant modal composition, were produced repeatedly beneath an area of hundreds of square kilometers during a period that may have lasted less than 130 000 years. Although not impossible, this scenario seems somewhat improbable.

Temperatures of about 800 °C determined using phenocrysts seem relatively high for porphyritic, high-silica rhyolite magma, unless the magma is volatile (H_2O, F, Cl) poor. Comparison of this temperature with those measured during experiments by Tuttle and Bowen (1958) in the system $NaAlSi_3O_8$-$KAlSi_3O_8$-SiO_2-H_2O suggests that either the Taylor Creek Rhyolite magma was H_2O undersaturated at an unspecified depth, or that it was H_2O saturated, but at such shallow depth that the H_2O content was quite low and thus had little effect in depressing liquidus temperature. Minor extrapolation of the experimental data of Tuttle and Bowen (1958) suggests a liquidus temperature of about 800 °C for the H_2O-saturated granitic system at a pressure of about 0.5 kbar.

That two-feldspar temperatures calculated from the Fuhrman and Lindsley (1988) geothermometer increasingly diverge from those of the Fe-Ti-oxide geothermometer as pressure is reduced below 2 kbar argues against a shallow magma reservoir. On the other hand, temperature difference between other two-feldspar geothermometers and the Fe-Ti-oxide geothermometer (Tables 3 and 4) is reduced with pressure below 2 kbar. However, two-feldspar geothermometry and associated geobarometry are almost certainly too inaccurate to resolve the issue (Grunder and Boden, 1987).

Application of the experimental results of Tuttle and

Bowen (1958) to the Taylor Creek Rhyolite is limited by the fact that the composition of the natural system differs somewhat from that of the experimental system. Such constituents as MgO (averages 0.14 wt%), CaO (0.29), and $Fe_2O_3^*$ (total Fe) (1.12) are present in concentrations low enough to encourage comparisons between the natural and synthetic magmas, but a relatively high F content in Taylor Creek Rhyolite indicates greatly differing volatile constituents for the two systems. Christiansen et al. (1986) report 0.38 wt% F; our unpublished whole-rock data suggest about 0.3%. Nonetheless, the effects of F on the liquidus and solidus of rhyolitic magmas are broadly similar to those of H_2O (Kovalenko, 1979; Manning, 1981; Dingwell et al., 1985), and thus the application of the experimental results of Tuttle and Bowen (1958) may indeed apply to the Taylor Creek Rhyolite. If so, and if the presence of pyroclastic products as part of an eruptive cycle is interpreted to indicate volatile saturation of the magma at the depth where phenocrysts grew, then the upper part of the reservoir was at only about 1.5 km during the formation of the lava field. Alternatively, phenocrysts may have grown at greater depth, in which case pyroclastic deposits reflect volatile saturation only near and at the surface during eruption.

Whitney (1988) summarized experimental results for granitic systems and textural features of granites and extrusive equivalents that are consistent with the scenario that Taylor Creek Rhyolite magma was not H_2O saturated during phenocryst growth. He reports that cooling of H_2O-undersaturated granitic magma should result in uniformly coarse-grained rock (with a quenched groundmass if quickly erupted), and primary magmatic quartz and sanidine crystals should exhibit resorption textures (Whitney, 1988). These are ubiquitous characteristics of the Taylor Creek Rhyolite. In addition, consideration of the experimental results for Cape Ann Granite of Massachusetts, whose major-element composition is nearly identical to that of Taylor Creek Rhyolite, suggests that Taylor Creek phenocrysts grew in magma that contained about 2.5 wt% H_2O (Whitney, 1988, Table 2 and Figure 4). Independent evidence of the volatile species and total volatile content of Taylor Creek Rhyolite magma is being sought through attempts to analyze glass inclusions in quartz phenocrysts.

Meanwhile, we conclude that the phenocrysts in Taylor Creek Rhyolite grew within a single reservoir of magma of nearly constant major-element composition, and that, as suggested by the areal distribution of vents, this reservoir was at least 20 km by 50 km in plan-view dimensions. The temperature at which phenocrysts grew was about 800 °C; the depth of the upper part of the reservoir was at least 1.5 km, and perhaps considerably greater if the magma was H_2O undersaturated, as we tentatively infer.

Acknowledgments

We thank Charles R. Bacon for help with analysis and interpretation of Fe-Ti oxides and for critical review of the text, which led to substantial improvement of the paper. Additional reviews by Gail Mahood, John S. Pallister, and Clay Conway resulted in improvements to an early version of the manuscript.

References cited

Andersen, D.J., and Lindsley, D.H. (1988) Internally consistent solution models for Fe-Mg-Mn-Ti oxides. American Mineralogist, 73, 714–726.

Bacon, C.R., and Hirshmann, M.M. (1988) Mg/Mn partitioning as a test for equilibrium between coexisting Fe-Ti oxides. American Mineralogist, 73, 57–61.

Bence, A.E., and Albee, A.L. (1968) Empirical correction factors for the electron microanalysis of silicates and oxides. Journal of Geology, 76, 382–403.

Christiansen, E.H., Sheridan, M.F., and Burt, D.M. (1986) The geology and geochemistry of Cenozoic topaz rhyolites from the western United States. Geological Society of America Special Paper 205, 82 p.

Correa, B.P. (1981) The Taylor Creek Rhyolite and associated tin deposits, southwestern New Mexico. 105 p. M.S. thesis, Arizona State University, Tempe, Arizona.

Dalrymple, G.B., and Duffield, W.A. (1988) High precision $^{40}Ar/^{39}Ar$ dating of Oligocene rhyolites from the Mogollon-Datil volcanic field using a continuous laser system. Geophysical Research Letters, 15, no. 5, 463–466.

Dingwell, D.B., Scarfe, C.M., and Cronin, D.J. (1985) The effect of fluorine on viscosities in the system Na_2O-Al_2O_3-SiO_2: Implications for phonolites, trachytes, and rhyolites. American Mineralogist, 70, 80–87.

Duffield, W.A. (in press) Eruptive fountains of silicic magma and their possible effects on the tin content of fountain-fed lavas. Geological Society of America Special Paper 246.

Duffield, W.A., Richter, D.H., and Priest, S.S. (1987) Preliminary geologic map of the Taylor Creek Rhyolite, Catron and Sierra Counties, New Mexico. U.S. Geological Survey Open-file Report 87-515, 1:50000.

Eggleston, T.L. (1987) The Taylor Creek District, New Mexico: Geology, petrology, and tin deposits. 473 p. Ph.D. thesis, New Mexico Institute of Mining and Technology, Socorro, New Mexico.

Eggleston, T.L., and Norman, D.I. (1986) A summary of the geology, geochemistry, and tin occurrences in the Black Range, New Mexico. New Mexico Geological Society Guidebook, 37th Field Conference, 173–177.

Elston, W.E. (1984) Mid-Tertiary ash flow tuff cauldrons, southwestern New Mexico. Journal of Geophysical Research, 89, 8733–8750.

Fries, C. Jr., and Butler, A.P. (1943) Geologic map of the Black Range tin district, New Mexico. U.S. Geological Survey Open-file Map, 1:62500.

Fuhrman, M.L., and Lindsley, D.H. (1988) Ternary feldspar modeling and thermometry. American Mineralogist, 73, 201–215.

Grunder, A.L., and Boden, D.R. (1987) Comment on "... Magmatic conditions of the Fish Canyon Tuff, central San Juan volcanic field, Colorado," by Whitney and Stormer (1985). Journal of Petrology, 28, part 4, 737–746.

Haselton, H.T. Jr., Hovis, G.L., Hemingway, B.S., and Robie, R.A. (1983) Calorimetric investigation of the excess entropy of mixing in analbite-sanidine solid solutions: Lack of evidence for Na, K short-range order and implications for two-feldspar geothermometry. American Mineralogist, 68, 398–413.

Kovalenko, N.I. (1979) An experimental study of formation of rare-metal Li-F granites. Nauka, Moscow, 152 (in Russian).

Lawrence, V.A. (1985) A study of the Indian Peaks tin-bearing rhyolite dome-flow complex, northern Black Range, New Mexico. 112 p. M.S. thesis, University of Colorado, Boulder, Colorado.

Manning, D.A.C. (1981) The effect of fluorine on liquidus phase relationships in the system Qz-Ab-Or with excess water at 1 kbar. Contributions to Mineralogy and Petrology, 76, 206–215.

Maxwell, C.H., Foord, E.E., Oakman, M.R., and Harvey, D.B. (1986) Tin deposits in the Black Range tin district. New Mexico Geological Society Guidebook, 37th Field Conference, 273–281.

McIntosh, W.C., Sutter, J.F., Chapin, C.E., Osburn, G.R., and Ratte, J.C. (1986) A stratigraphic framework for the eastern Mogollon-Datil volcanic field based on paleomagnetism and high-precision $^{40}Ar/^{39}Ar$ dat-

ing of ignimbrites—A progress report. New Mexico Geological Society Guidebook, 37th Field Conference, 183–195.

Price, J.G. (1985) Ideal site mixing in solid solutions, with an application to two-feldspar geothermometry. American Mineralogist, 70, 696–701.

Ratte, J.C. (1987) Some comparisons of the San Juan and Mogollon-Datil volcanic fields, Colorado and New Mexico. Geological Society of America Abstracts with Programs, 19, no. 5, 328.

Reece, C., Ruiz, J., Duffield, W.A., and Patchett, P.J. (in press) Origin of Taylor Creek Rhyolite magma, Black Range, New Mexico, based on Nd-Sr isotope studies. Geological Society of America Special Paper 246.

Rye, R.O., Lufkin, J.L., and Wasserman, M.D. (in press) Genesis of the rhyolite-hosted tin occurrences in the Black Range, New Mexico, as indicated by stable isotope studies. Geological Society of America Special Paper 246.

Seck, H.A. (1971) The effect of pressure on the composition of coexisting alkali feldspars and plagioclases in the system $NaAlSi_3O_8$-$KAlSi_3O_8$-$CaAl_2Si_2O_8$-H_2O. Contributions to Mineralogy and Petrology, 31, 67–86.

Smith, R.L. (1960) Zones and zonal variations in welded ash flows. U.S. Geological Survey Professional Paper 354-F, 149–159.

Smith, R.L., and Shaw, H.R. (1979) Igneous-related geothermal systems. U.S. Geological Survey Circular 790, 12–17.

Stormer, J.C. (1975) A practical two-feldspar geothermometer. American Mineralogist, 60, 667–674.

——— (1983) The effects of recalculation on estimates of temperature and oxygen fugacity from analyses of multicomponent iron-titanium oxides. American Mineralogist, 68, 586–594.

Tuttle, O.F., and Bowen, N.L. (1958) Origin of granite in the light of experimental studies in the system $NaAlSi_3O_8$-$KAlSi_3O_8$-SiO_2-H_2O. Geological Society of America Memoir 74, 153 p.

Whitney, J.A. (1988) The origin of granite: The role and source of water in the evolution of granitic magmas. Geological Society of America Bulletin, 100, 1886–1897.

Whitney, J.A., and Stormer, J.C. (1977) The distribution of $NaAlSi_3O_8$ between coexisting microcline and plagioclase and its effects on geothermometric calculations. American Mineralogist, 62, 687–691.

MANUSCRIPT RECEIVED SEPTEMBER 26, 1989
MANUSCRIPT ACCEPTED JULY 16, 1990